Pharmacological MRI to investigate the functional selectivity of 5-HT1A receptor biased agonists

Benjamin Vidal, Radu Bolbos, Jérôme Redouté, Jean-Baptiste Langlois, Nicolas Costes, Adrian Newman-Tancredi, Luc Zimmer

Pharmacological MRI to investigate the functional selectivity of 5-HT$_{1A}$ receptor biased agonists

Benjamin Vidal[a], Radu Bolbos[b], Jérôme Redouté[b], Jean-Baptiste Langlois[b], Nicolas Costes[b], Adrian Newman-Tancredi[c], Luc Zimmer[a,b,d,e]

[a]Université de Lyon, Lyon Neuroscience Research Center, INSERM, CNRS, Bron, France

[b]CERMEP-Imagerie du Vivant, Bron, France

[c]Neurolixis SAS, Castres, France

[d]Hospices Civils de Lyon, Lyon, France

[e]National Institute for Nuclear Science and Technology, Saclay, France

Corresponding Author: Luc Zimmer. Address: CERMEP, Groupement Hospitalier Est, 59 Boulevard Pinel, F-69677 Bron, France. E-mail: luc.zimmer@univ-lyon1.fr

Abstract

The emerging concept of “biased agonism” denotes the phenomenon whereby agonists can preferentially direct receptor signalling to specific intracellular responses among the different transduction pathways, thus potentially avoiding side effects and improving therapeutic effects. The aim of this study was to investigate biased agonism by using pharmacological magnetic resonance imaging (phMRI). The cerebral blood oxygen level dependent (BOLD) signal changes induced by increasing doses of two serotonin 5-HT_{1A} receptor biased agonists, NLX-112 and NLX-101, were mapped in anaesthetized rats. Although both compounds display high affinity, selectivity and agonist efficacy for 5-HT_{1A} receptors, NLX-101 is known to preferentially activate post-synaptic receptors, whereas NLX-112 targets both pre- and post-synaptic receptors. We used several doses of agonists in order to determine if the regional selectivity of NLX-101 was dose-dependent. NLX-112 and NLX-101 induced different positive and negative hemodynamic changes patterns at equal doses. Importantly, NLX-101 had no significant effect in regions expressing pre-synaptic receptors contrary to NLX-112. NLX-112 also produced higher BOLD changes than NLX-101 in the orbital cortex, the somatosensory cortex, and the magnocellular preoptic nuclei. In other regions such as the retrosplenial cortex and the dorsal thalamus, the drugs had similar effects. In terms of functional connectivity, NLX-112 induced more widespread changes than NLX-101. The present phMRI study demonstrates that two closely-related agonists display notable differences in their hemodynamic “fingerprints”. These data support the concept of biased agonism

at 5-HT_{1A} receptors and raise the prospect of identifying novel therapeutics which exhibit improved targeting of brain regions implicated in neuropsychiatric disorders.

Keywords: 5-HT_{1A} receptor, NLX-112, NLX-101, biased agonism, phMRI, fMRI

Abbreviations: Amy = Amygdala; BOLD: blood oxygen level-dependent; Cing Ctx = Cingulate cortex; Coll = Colliculus; fMRI: functional magnetic resonance imaging; FWE: familywise error rate; GIRK: G protein-coupled inwardly-rectifying potassium; Hip = Hippocampus; Hyp = Hypothalamus; Ins = Insula; MCPO: magnocellular preoptic nuclei; Orb Ctx = Orbital cortex; phMRI: pharmacological magnetic resonance imaging; PET: positron emission tomography; rCBV: relative cerebral blood volume; Retro Ctx = Retrosplenial cortex; ROI: region of interest; Sept = Lateral septum; SMS Ctx = Somatosensory cortex; SPM: statistical parametric mapping; Striat = Striatum; Sub = Subiculum; Thal = Thalamus; Vis Ctx = Visual cortex.

Introduction

Serotonin, or 5-hydroxytryptamine (5-HT), plays a critical role in the central nervous system by acting through multiple receptor subtypes. Among these, the 5-HT_{1A} receptor exhibits considerable functional importance and has attracted interest as a target for pharmacotherapy of psychiatric or neurodegenerative disorders (Lacivita et al., 2012). 5-HT_{1A} receptors are expressed both as autoreceptors in the raphe nuclei, where they exert inhibitory influence on serotonergic tone (Andrade et al., 2015), and as post-synaptic heteroreceptors in cortex, hippocampus, lateral septum and hypothalamus (Lanfumey and Hamon, 2000). 5-HT_{1A} heteroreceptors can be located on different neuronal populations such as GABAergic, glutamatergic or cholinergic neurons (Santana et al., 2004; Luttgen et al., 2005). In addition to this regional diversity, 5-HT_{1A} receptors can induce a wide range of intracellular responses (Polter and Li, 2010). As G protein-coupled receptors (GPCR) that interact with inhibitory G-proteins (Gi/o), they mediate inhibition of adenylyl cyclase, resulting in decreased cyclic adenosine monophosphate (cAMP) production and protein kinase A (PKA) activity. Stimulation of 5-HT_{1A} receptors also activates G protein-coupled inwardly-rectifying potassium (GIRK) channels, and growth factor-associated ERK phosphorylation pathways. Notably, these transduction pathways can differ between brain regions (Newman-Tancredi, 2011), which is likely related to coupling with different G-protein subtypes (Mannoury la Cour et al., 2006). For instance, 5-HT_{1A} autoreceptors are prominently coupled to G protein-activated inwardly rectifying potassium (GIRK) channels in 5-HT neurons (Montalbano et al., 2015) whereas other signalling pathways are associated with 5-HT_{1A} heteroreceptors, such as activation of ERK1/2 phosphorylation (Mogha et al., 2012). The recent paradigm of “biased agonism”, or “functional selectivity”, states that some agonists are able to

preferentially stimulate specific intracellular signalling pathways among the different pathways interacting with the same receptor (Kenakin and Christopoulous, 2013; Berg and Clarke, 2006). In the context of the pharmacotherapy of CNS disorders, this opens the possibility of targeting 5-HT_{1A} receptors in specific brain regions depending on their coupling with different pathways (Newman-Tancredi, 2011), in order to optimize therapeutic benefit. For instance, preferential activation of post-synaptic cortical receptors *versus* autoreceptors should be useful to treat cognitive dysfunction (Depoortere et al., 2010).

In this context, we focus here on two 5-HT_{1A} biased agonists, NLX-101 (a.k.a. F15599) and NLX-112 (a.k.a. F13640 or befiradol). Both display high affinity, efficacy and specificity at 5-HT_{1A} receptors, although *in vitro* studies show that they preferentially stimulate different signalling pathways (Newman-Tancredi et al., 2009; Newman-Tancredi et al., 2017). Preclinical studies also suggest that NLX-101 is able to preferentially target post-synaptic 5-HT_{1A} receptors at low doses, in particular in cortical regions (Newman-Tancredi et al., 2009; Llado-Pelfort et al., 2010). In contrast, although NLX-112 is able to activate cortical 5-HT_{1A} receptors, it also potently activates autoreceptors (Buritova et al., 2009; Llado-Pelfort et al., 2012a). Consequently, the two ligands are being developed as drug candidates for different indications, respectively breathing irregularity and cognitive deficits in Rett syndrome (Levitt et al., 2013), and L-DOPA-induced dyskinesia in Parkinson's disease (Iderberg et al., 2015; McCreary et al., 2016). However, the previous studies that demonstrated regional selectivity of NLX-101 and NLX-112 in rat brain used invasive and regionally-limited techniques, such as electrophysiology, microdialysis or immunohistochemistry. Thus, the potentially broader 'biased agonism' of NLX-101 and NLX-112 in the whole brain *in vivo* remains currently unexplored.

In this regard, pharmacological MRI (phMRI) is a promising tool as it enables mapping of the functional effect of ligands in the entire brain in a non-invasive way, thus providing a translational method to evaluate the functional selectivity of different agonists. In a previous study, we showed that 5-HT_{1A} biased agonists can induce different brain activation patterns in phMRI (Becker et al., 2016). However, we did not investigate dose-effect relationships on the phMRI pattern, a crucial parameter in relation to the selective targeting of 5-HT_{1A} receptor subpopulations (Llado-Pelfort et al., 2010); furthermore, the ligands we previously tested display very different receptor binding affinities, which precluded direct comparisons using an identical dose range. Here, we used phMRI to compare NLX-112 and NLX-101 at the same increasing doses (0.16/0.32/0.63 mg/kg i.p.). We aimed to map the central effects of the agonists and sought to determine whether NLX-101 exhibits distinct brain hemodynamic effects and brain connectivity relationships compared to NLX-112.

1. Material and methods

1.1 Animals and procedures

Nineteen male Sprague-Dawley adult rats (Charles River Laboratories, France) weighing 300 ± 50g were used in this study. The animals were hosted in standard temperature and humidity conditions with a 12h/12h light/dark cycle, with food and water *ad libitum*. All experiments were performed in accordance with European guidelines for care of laboratory animals (2010/63/EU) and were approved by the Animal Use Ethics Committee of the University of Lyon (Université Claude Bernard Lyon 1). The animal species and strain were chosen according to previous microdialysis or ex vivo studies conducted with NLX-101 and NLX-112 (Llado-Pelfort

et al., 2010; Llado-Pelfort et al., 2012a; Newman-Tancredi et al., 2009; Buritova et al., 2009).

Anesthesia induction was performed with a mixture of 4% isoflurane (AErane, Baxter France) and air (1L/min), then lowered to 2% isoflurane during the catheterization procedure. The catheter was maintained by ligation to the abdominal wall and a tube was connected to carry out pharmacological agents or saline injections during the scan. The animals were placed on prone position in a dedicated plastic holder (Bruker Biospec Animal Handling Systems, Germany), adapted with a stereotactic system allowing animal's head immobilization. The anesthesia was maintained at 2% isoflurane during the MRI acquisition. The body temperature was maintained at 37 ± 0.2 °C by means of a temperature-controlled water circuit integrated in the dedicated holder. The respiratory rate was also monitored during the acquisition.

1.2 Experimental design

The animals were divided into two groups, one for each molecule (n=10 for NLX-101 and n=9 for NLX-112: one animal was lost during the protocol). All rats were scanned under four conditions in a randomized order: a saline (NaCl 0.9 %) injection, and three increasing doses (0.16 / 0.32 / 0.63 mg/kg) of either NLX-112 or NLX-101. For the same animal, each acquisition were separated by at least 3 days, based on previous data showing that plasma half-lives of NLX-112 and NLX-101 are about 1 to 3 hours (Bardin et al., 2005 and unpublished data).

1.3 phMRI protocol

The MRI protocol was carried out on a 7-Tesla Bruker Biospec MR system (Bruker BiospinGbmH, Germany). A transmitting body coil (outer diameter, 112 mm and inner diameter, 72 mm) and a receive-only surface coil (25 mm of diameter) were used for

rat brain image acquisitions. A 2D anatomical T2-RARE image (Rapid Acquisition with Relaxation Enhancement) was obtained with the following parameters: echo time (TE): 69.1 ms, repetition time (TR): 5000 ms, field of view: 3 × 1.5 cm^2, matrix 256 × 128 pixels, spatial resolution: 117 μm^2, RARE factor: 8, acquisition time: 4 minutes. 14 contiguous slices of 1.5-mm thickness were acquired, covering the whole rat brain. To measure local BOLD variations during pharmacological stimulations, a T2* (Echo Planar Imaging) sequence was used with the following parameters: TE/TR: 25/3000 ms, matrix 128 × 64 pixels, spatial resolution: 234 μm^2. 14 slices were acquired with the identical geometry of the anatomical T2-RARE scan. Each fMRI session lasted one hour, corresponding to 1200 repetitions. The pharmacological challenge was performed 15 minutes after the beginning, resulting in 15 minutes of baseline period (300 repetitions) and 45 minutes of post-injection period (900 repetitions). The injected volumes of the saline or agonist solutions were set at 600 µL, immediately followed by a 600 µL saline flush.

1.4 Data preprocessing

Data were analyzed using Statistical Parametric Mapping software (SPM12, The Wellcome Trust Center for Neuroimaging, London, UK). Three preprocessing steps were performed: (1) images realignment using a spatial cross-correlation algorithm, ensuring motion correction and enabling us to realign images from all acquisitions together, (2) spatial normalization using a standardized MRI template (Lancelot et al., 2014), and (3) spatial smoothing using anisotropic Gaussian filter [0.8 × 0.8 × 0.8 mm Full Width at Half Maximum (FWHM)]. This preprocessing enabled inter-subject averaging. Each step of the preprocessing was verified by visually checking the quality of images.

1.5 Regional time course responses

For each scan, the time courses of the BOLD signal were extracted from different regions of interest (ROIs) on the 1200 pre-processed images. These regions were either automatically delineated using an already available rat brain atlas normalized on the same MRI template (Lancelot et al., 2014), or manually drawn according to the results of the voxel-based analysis (insula, MCPO, retrosplenial cortex, colliculus, orbital cortex, septum, somatosensory cortex, visual cortex, subiculum).

1.6 Statistical analysis

1.6.1 Voxel-based analysis

For each rat, a first-level analysis (intra-subject) was performed for all experimental conditions. The 1200 repetitions per session were divided into four time bins. The 300 baseline repetitions (15 min) were defined as the first time bin (T0). The 900 post-injection repetitions (15 min) were divided into 3 time bins of 300 repetitions each (T1 to T3). The 15-minutes periods were defined based on previous data showing that the Tmax of NLX-112 in plasma occurs at about 15 minutes (Bardin et al., 2005). The four time bins were introduced into a SPM block design using a General Linear Model (GLM) approach. The mean signals measured in ventricles, obtained by the regional extraction using the atlas, was taken as regressor of non-interest to correct for possible systemic fluctuations that could impact the BOLD signal (Mandeville et al., 2014). We made the assumption that the BOLD signal changes occurring in ventricles are non-specific and mostly due to systemic fluctuations (Birn et al., 2009). The respiratory rate was also used as a regressor of non-interest. No global scaling was performed. This first-level analysis resulted in three first-level parametric contrast images per subject and per condition,

corresponding to contrasts $[Tn - T0]_{condition}$. Second-level analyses were carried out to determine significant variations of BOLD signal across subjects at a voxel level for each dose of agonist compared to control. BOLD increase maps were generated using the contrasts $[(\text{Post-injection} - \text{Baseline})_{Agonist} - (\text{Post-injection} - \text{Baseline})_{NaCl}]$. BOLD decrease maps were generated using the reverse contrasts $[(\text{Post-injection} - \text{Baseline})_{NaCl} - (\text{Post-injection} - \text{Baseline})_{Agonist}]$. This second-level used repeated measure analysis of variance (ANOVA) with the time bins contrasts as between-group factor (molecule versus saline injections) for each time bin. A significant threshold was set up at $p<0.001$ with a FWE correction for multiple comparisons at $p<0.05$. A third-level analysis was also performed to directly compare NLX-101 and NLX-112 effects at the same doses, using the contrasts $[(\text{Post-injection} - \text{Baseline})_{NLX-112} - (\text{Post-injection} - \text{Baseline})_{NaCl}] - [(\text{Post-injection} - \text{Baseline})_{NLX-101} - (\text{Post-injection} - \text{Baseline})_{NaCl}]$ and reverse contrasts $[(\text{Post-injection} - \text{Baseline})_{NLX-101} - (\text{Post-injection} - \text{Baseline})_{NaCl}] - [(\text{Post-injection} - \text{Baseline})_{NLX-112} - (\text{Post-injection} - \text{Baseline})_{NaCl}]$. A significant threshold was set up at $p<0.001$ with FWE correction ($p<0.05$).

1.6.2 Regions of interest analyses

For each acquisition, the mean BOLD signal in each ROI was averaged for the first 300 images (baseline) and the 900 latest images (post-injection). The results were then expressed in percentage of BOLD changes compared to the baseline, and averaged for each condition (the control conditions and the three doses of each agonist). The changes occurring after the injections of different doses of NLX-101 or NLX-112 were statistically compared to the injection of saline using a two-way ANOVA followed by Bonferroni's post-hoc tests (with correction for multiple comparisons) using Graphpad Prism 7 software. For direct comparisons between

NLX-101 and NLX-112, a two-way ANOVA with Tukey's multiple comparisons tests was used. The statistical significance was set at $p<0.05$.

A functional connectivity analysis was also performed on the same data. For each acquisition, temporal correlations were evaluated by measuring the Pearson correlation coefficient between the different BOLD signal curves for each pair of region during the 900 latest repetitions. The correlation matrix displaying the correlation coefficients for every pairs of regions was generated using Graphpad Prism 7. For each condition, the matrices were averaged to obtain mean correlation matrices. For all doses of NLX-101 or NLX-112, correlation coefficients were transformed by Fisher Z transformation in order to ensure a normal distribution, then statistically compared to the saline condition using a two-way ANOVA followed by Bonferroni's multiple comparisons post-hoc tests using Graphpad Prism 7. The statistical significance was set at $p<0.001$.

1.7 Drugs

NLX-112 (3-chloro-4-fluoro-phenyl)-[4-fluoro-4-{[(5-methyl-pyperidin-2-ylmethyl)-amino]-methyl} piperidin-1-yl]-methanone), i.e. befiradol or F13640, and NLX-101 (3-chloro-4-fluorophenyl)-[4-fluoro-4-[[(5-methylpyrimidin-2-yl)methylamino]methyl]piperidin-1-yl]methanone), i.e. F15599, were supplied by Neurolixis Inc. (Dana Point, CA, USA). Both drugs were administered i.p. in saline solution.

2. Results

2.1 Voxel-based analysis

The statistical maps of BOLD changes (increase or decrease) induced by the 5-HT_{1A} agonists injection were generated using SPM. The maps were established for each post-injection period at each dose of NLX-112 (Fig. 1-3) or NLX-101 (Fig. 4-6) at $p<0.001$ and FWE correction ($p<0.05$).

2.1.1 NLX-112

NLX-112 induced widespread changes of BOLD signal for every dose tested (Fig. 1-3). Significant BOLD increases were systematically found in an area spreading from the habenula (-3.00 mm) to the dorsal thalamus (-3.00/-5.40 mm), the retrosplenial cortex (-5.40/-6.60 mm) and the colliculi (-6.60/7.50 mm), that increased progressively in size and significance from T1 (first 15 minutes post-injection) to T3 (30 to 45 min post-injection). Other significant increases were found in the magnocellular preoptic nuclei (MCPO; +0.30/-1.20 mm). NLX-112 also produced an increase of BOLD signal in the cingulate cortex at 0.16 mg/kg (Fig. 1) and 0.32 mg/kg (Fig. 2), that was most obvious at T3. In addition, NLX-112 induced significant BOLD decreases. For all doses, negative responses were found in the orbital cortex (+3.90 mm), the lateral septum (+0.90/+0.30 mm), the somatosensory cortex (-3.00/-4.20 mm), the subiculum (-7.50 mm) and the brainstem. BOLD decreases were also systematically found at -1.20 mm from the bregma, and were located in the most ventral and lateral parts of the striatum and in the lateral globus pallidus (Fig. 2), or in the interstitial nucleus of the posterior limb of the anterior commissure (Fig. 1-3), depending on the different doses. BOLD signal decreases were also seen in the hypothalamus, namely the medial preoptic area at 0.16 mg/kg and 0.63 mg/kg, or the paraventricular area at 0.32 mg/kg. At 0.32 mg/kg, we also observed a significant decrease of BOLD signal in the dorsal raphe nucleus (-7.50 mm). All the observed

decreases followed similar kinetics and were mostly non-significant during the first minutes post-injection and became obvious after 15 minutes post-injection.

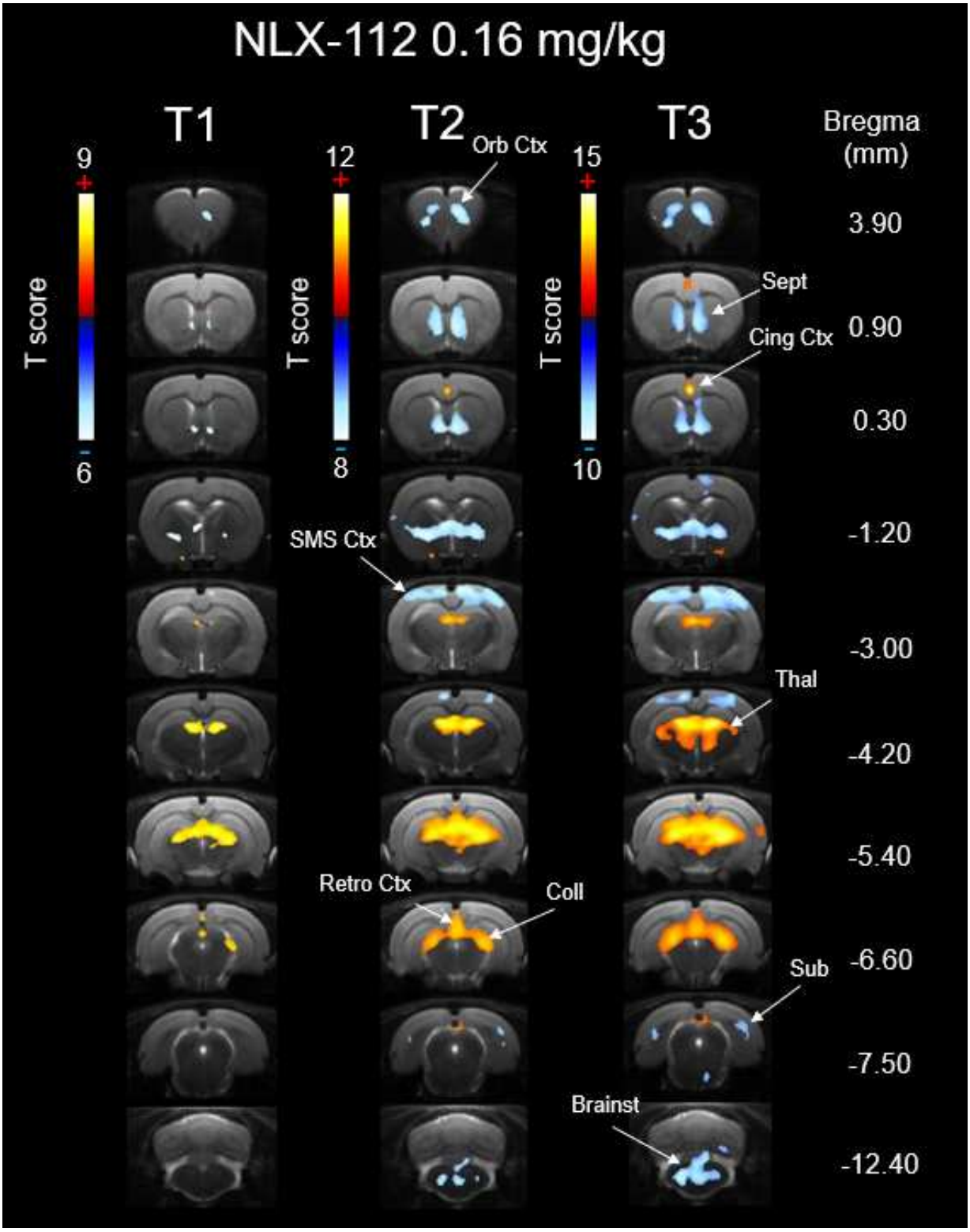
NLX-112 0.16 mg/kg
T1
T2
T3
Bregma (mm)
T score
9
6
12
8
15
10
Orb Ctx
Sept
Cing Ctx
SMS Ctx
Thal
Retro Ctx
Coll
Sub
Brainst
3.90
0.90
0.30
-1.20
-3.00
-4.20
-5.40
-6.60
-7.50
-12.40

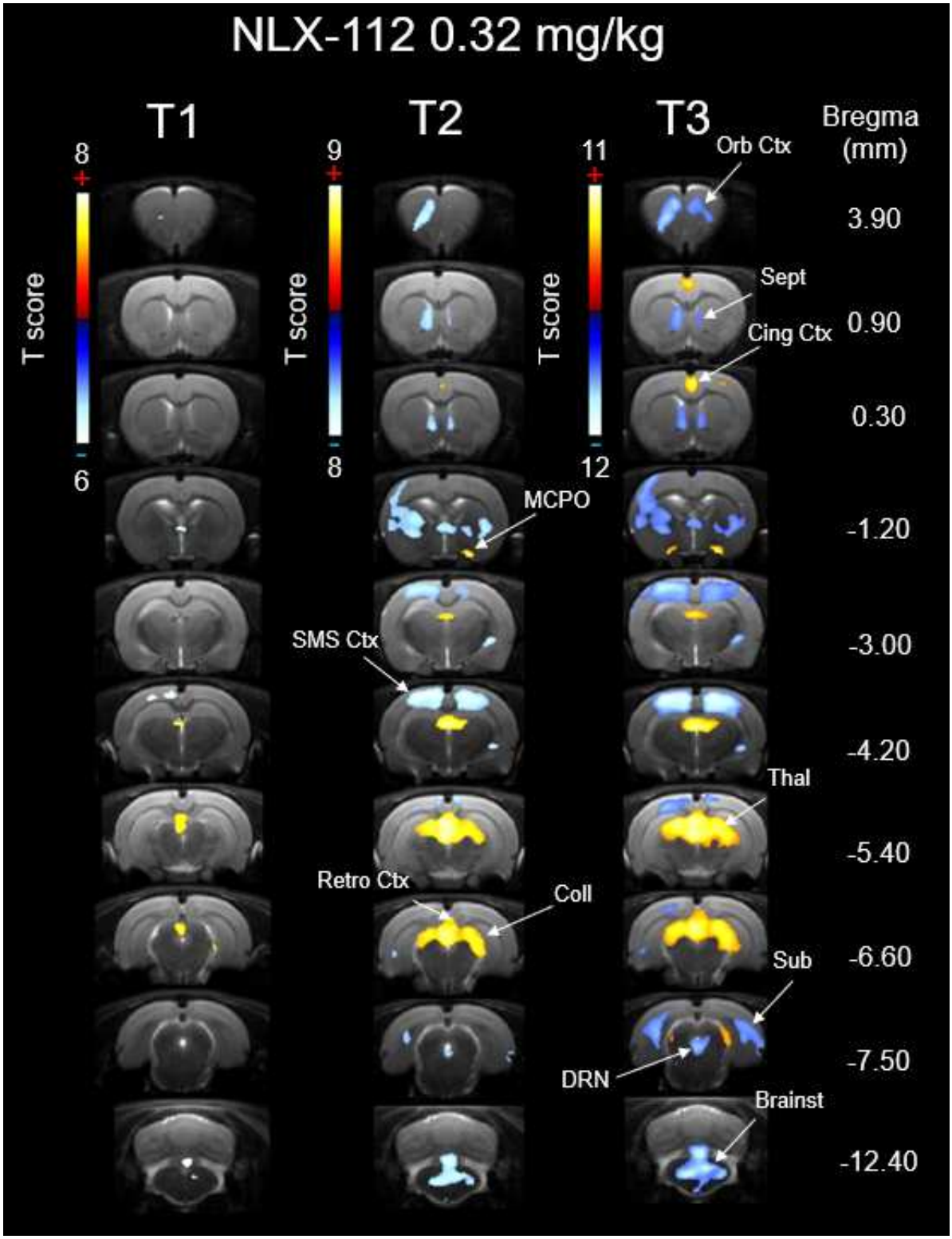
NLX-112 0.32 mg/kg
T1
T2
T3
Bregma (mm)
T score
8
6
9
8
11
12
Orb Ctx
3.90
Sept
Cing Ctx
0.90
0.30
MCPO
-1.20
SMS Ctx
-3.00
-4.20
Thal
-5.40
Retro Ctx
Coll
Sub
-6.60
DRN
-7.50
Brainst
-12.40

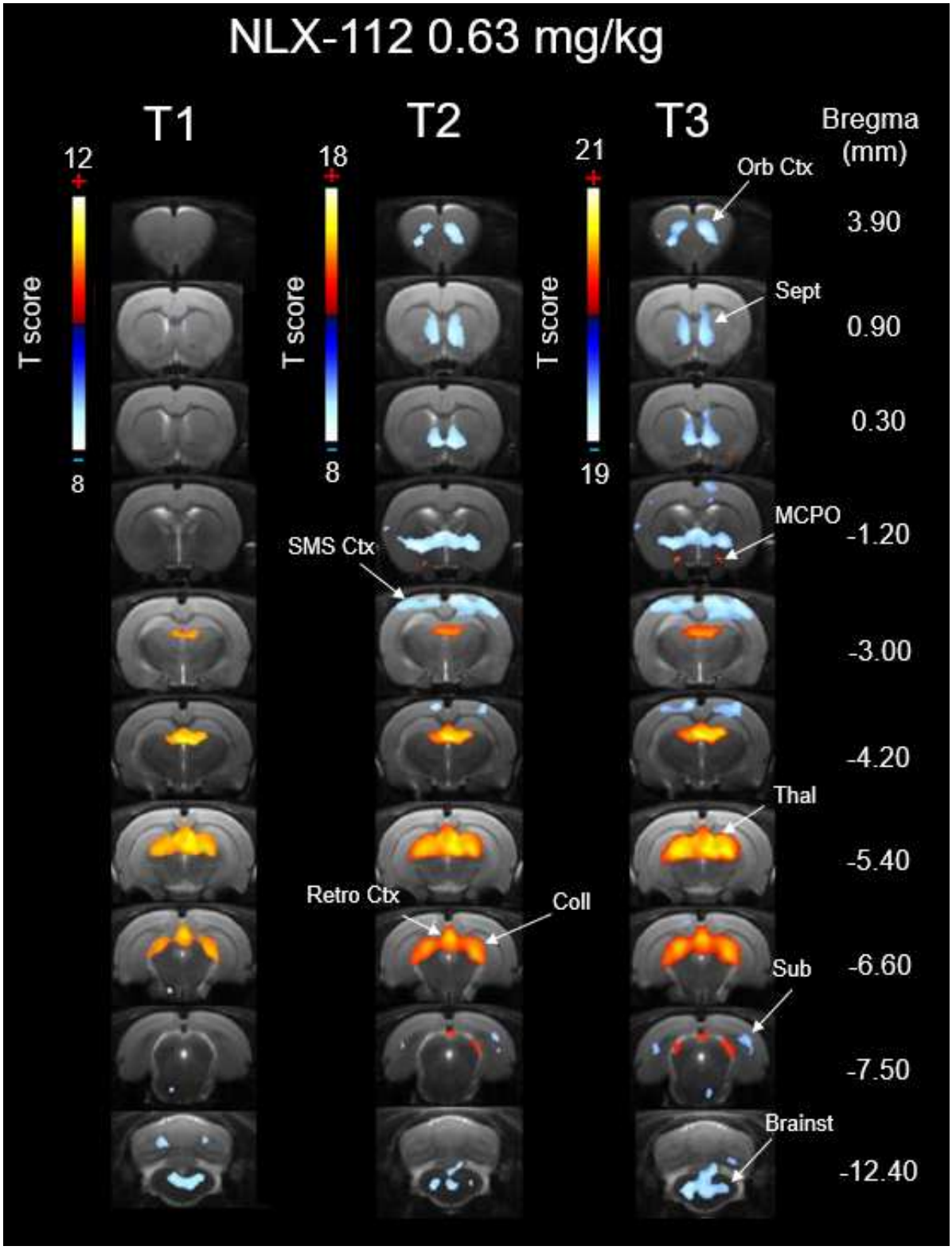

2.1.2 NLX-101

NLX-101 also induced positive and negative changes of BOLD signal for every dose tested (Fig. 4-6). Significant increases were found in large clusters spreading from

the habenula to the dorsal thalamus, the retrosplenial cortex, and the colliculi, and in the magnocellular preoptic nuclei, that increased progressively in size and significance from T1 to T3. A significant increase was also found in the cingulate cortex after 30 minutes post-injection at 0.16 mg/kg and 0.63 mg/kg of NLX-101. The patterns of significant decreases varied across the doses. At 0.16 mg/kg, a negative BOLD response was only found in the left somatosensory cortex. At 0.32 mg/kg, they were located in the lateral septum and the globus pallidus/paraventricular area (-1.20 mm). At 0.63 mg/kg, they were found in the orbital cortex and the somatosensory cortex/dorsal horn of the hippocampus (-3.00 mm).

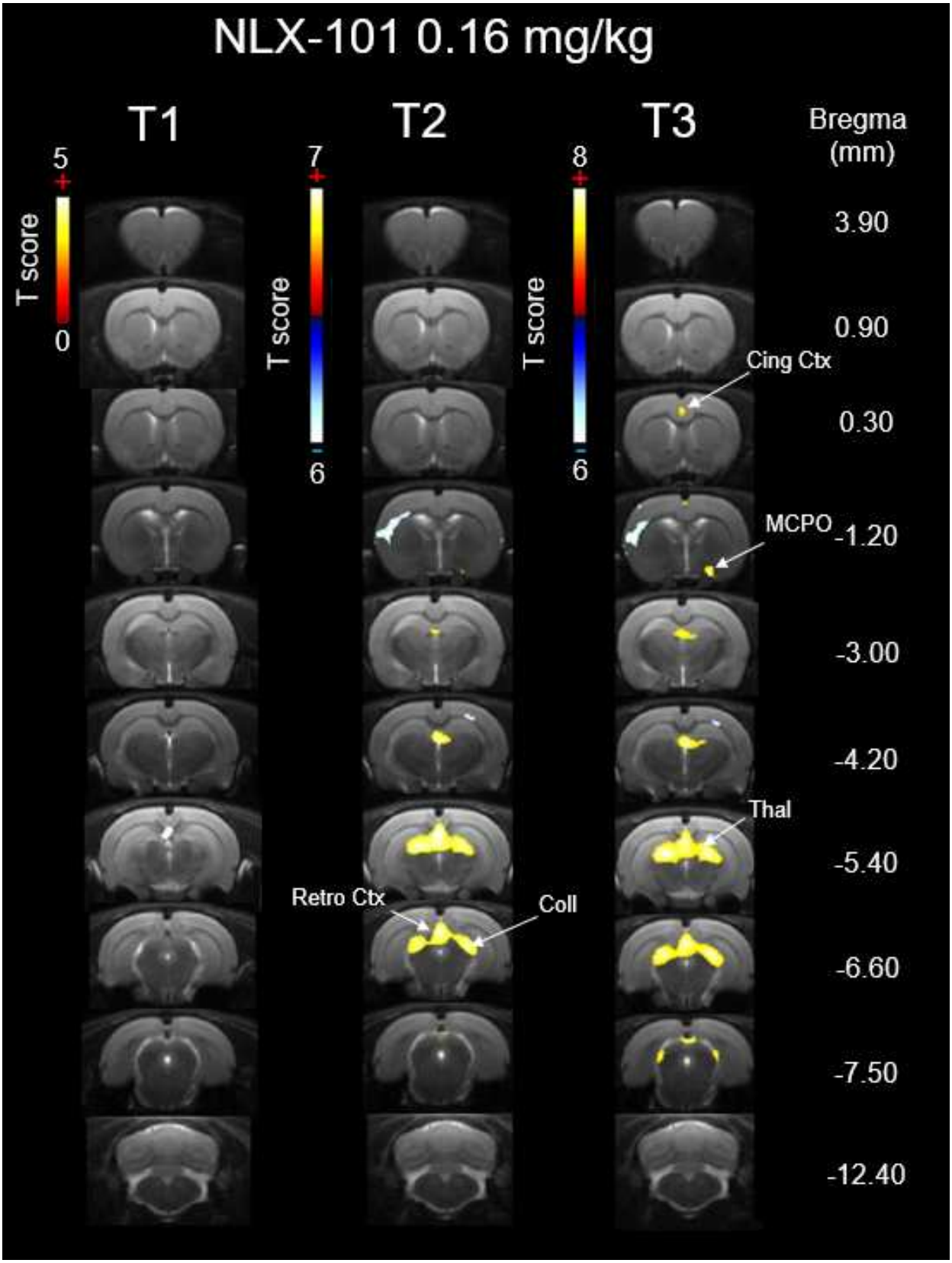
NLX-101 0.16 mg/kg
T1
T2
T3
Bregma (mm)
T score
5
0
7
6
8
6
3.90
0.90
Cing Ctx
0.30
MCPO
-1.20
-3.00
-4.20
Thal
-5.40
Retro Ctx
Coll
-6.60
-7.50
-12.40

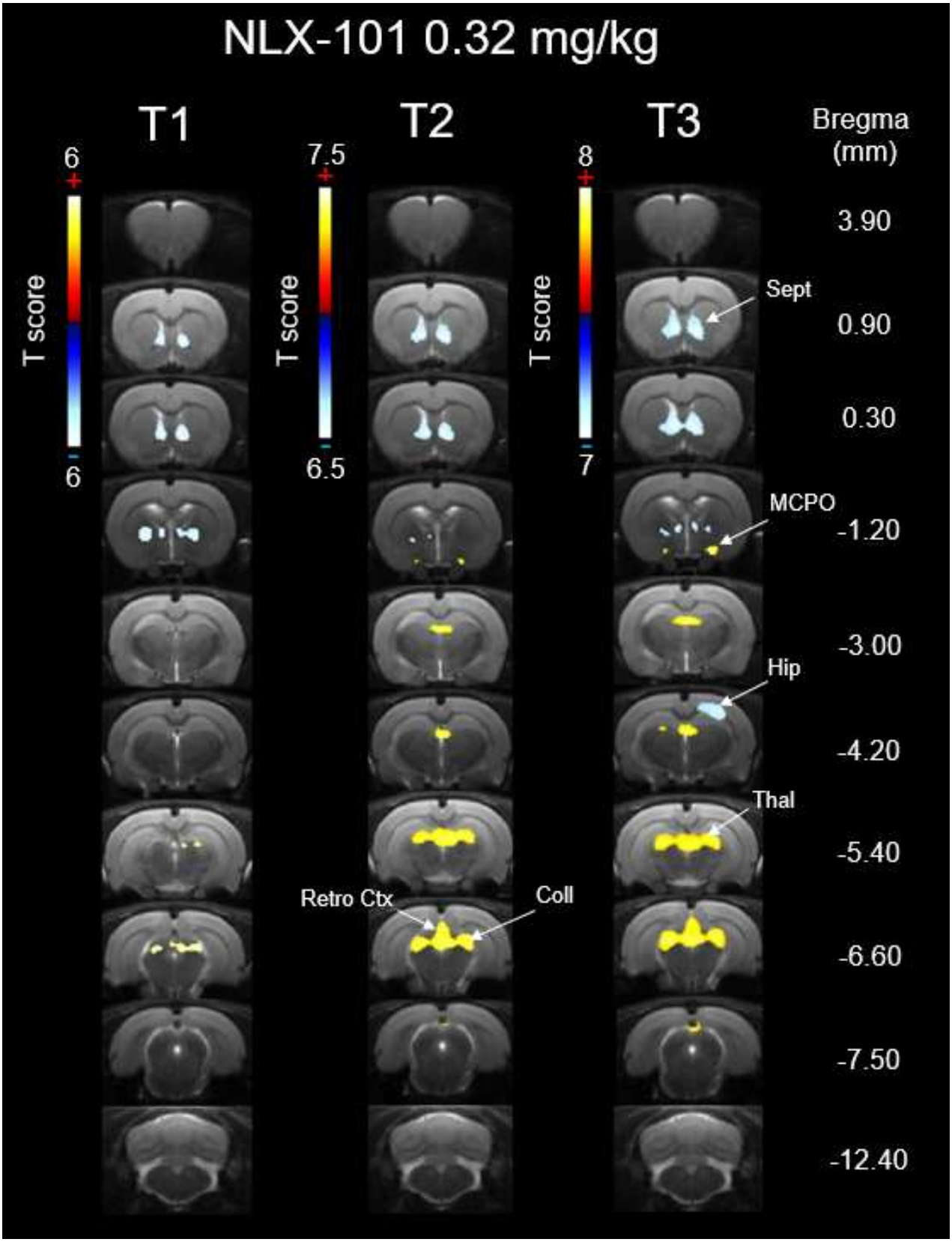

2.1.3 NLX-112 versus NLX-101

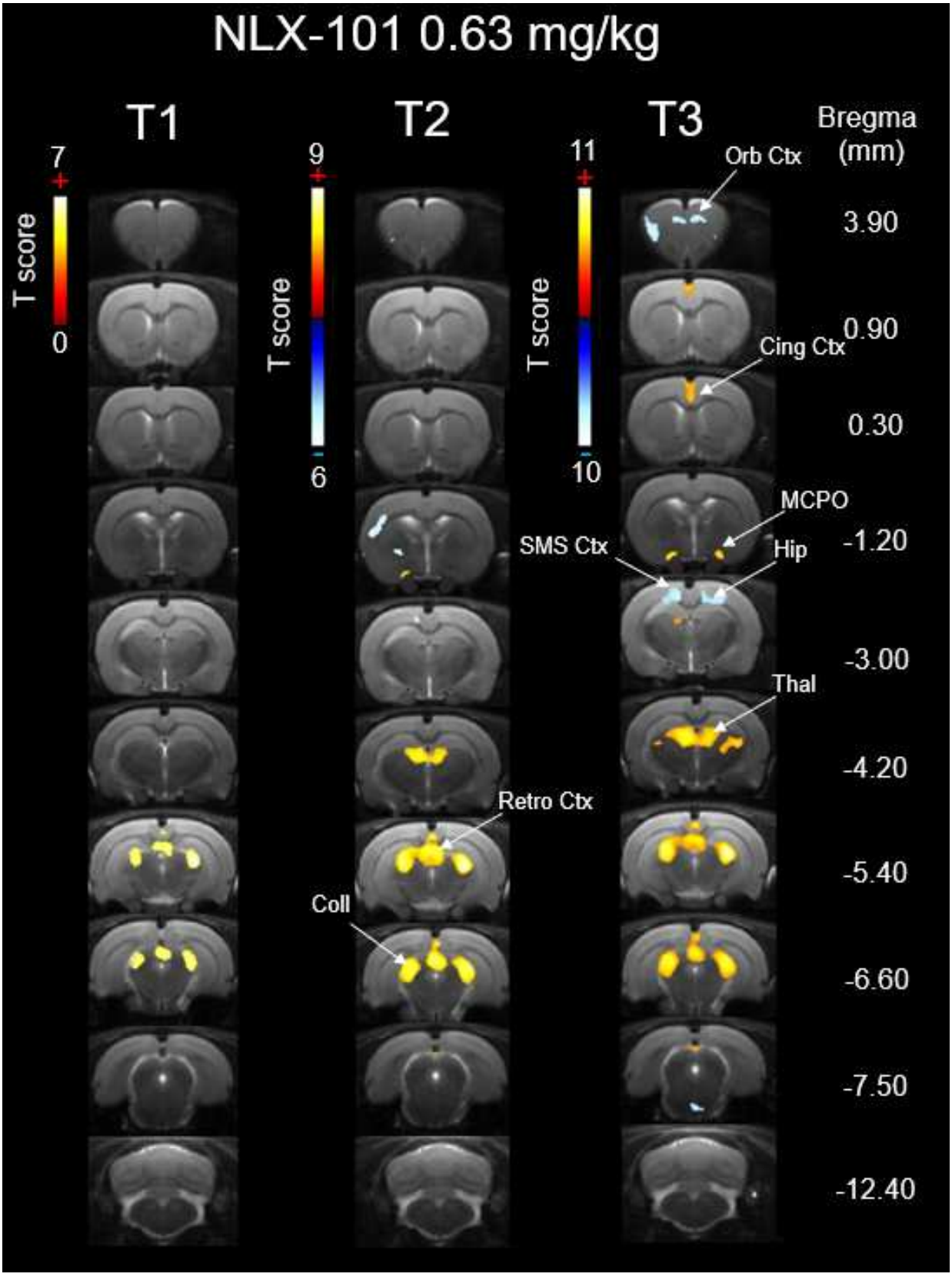
NLX-101 0.63 mg/kg
T1
T2
T3
Bregma (mm)
T score
7
0
9
6
11
10
Orb Ctx
Cing Ctx
MCPO
SMS Ctx
Hip
Thal
Retro Ctx
Coll
3.90
0.90
0.30
-1.20
-3.00
-4.20
-5.40
-6.60
-7.50
-12.40

The significant changes in BOLD signal compared to control condition were also directly compared between the agonists (see Fig. 7 for the differences in the T3 time period).

For the contrast [(NLX-112 – NaCl) – (NLX-101 – NaCl)], in green, only one cluster was observed in the right temporal cortex at 0.16 mg/kg. For the reverse contrast [(NLX-101 – NaCl) – (NLX-112 – NaCl)], in purple, the most important changes were found at 0.16 mg/kg. Significant clusters were found in various cortical areas, namely the anterior part of the retrosplenial cortex and few areas in the somatosensory cortex. Another cluster was found in a small area corresponding to the ventral part of the striatum and the right interstitial nucleus of the posterior limb of the anterior commissure. Few voxels were also detected in the rostral brainstem.

At 0.32 mg/kg, the only clusters were found in the most lateral parts of the frontal cortex and a small area of the ventral striatum, similarly to the previous dose. At 0.63 mg/kg, the significant differences were found in the left hypothalamus and brainstem.

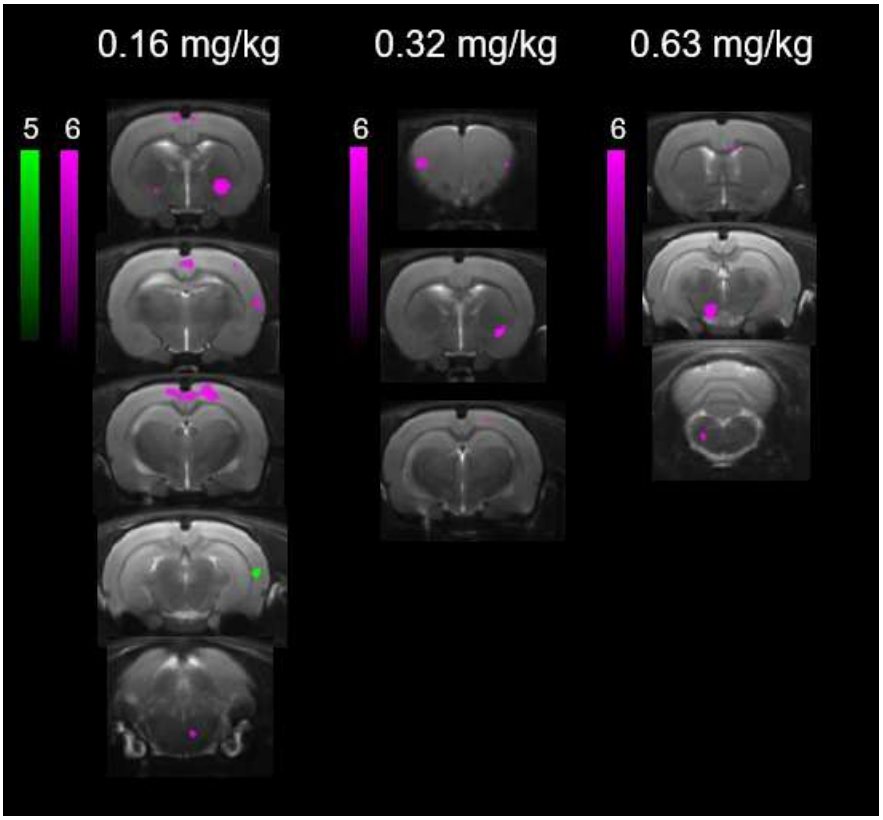

2.2. Region-of-interest analysis

2.2.1 NLX-112

The BOLD signal changes occurring after the injection of NLX-112 were extracted from the different regions of interest and statistically compared to the changes occurring after the injection of NaCl 0.9% (Fig. 8). The highest positive response was found in the MCPO, with an increase of 9% at 0.16 mg/kg, to nearly 12% at higher doses (all doses with $p<0.0001$). Other significant increases in BOLD signal were observed in the retrosplenial cortex and the thalamus, where increasing doses of NLX-112 induced a BOLD increase of 7.7%, 8.1%, and 8.4%, and 6.9%, 6.3% and 5.5%, respectively. Hence, changes in the retrosplenial cortex were proportional to the dose, whereas they decreased with the dose in the dorsal thalamus. In the

cingulate cortex a bell-shaped effect was observed, with the BOLD increase at 0.32 mg/kg being the only significant (+5.1%) . Other significant increases were found in the colliculi at 0.32 mg/kg and 0.63 mg/kg (+5.6% and +4.4%, respectively). Significant decreases in BOLD signal were found in the brainstem, that were proportional to the dose (from -5.9% to 9%), and in the orbital cortex, that were inversely proportional to the dose (from -7.1% to -4.4%). Another important BOLD decrease appeared in the hypothalamus at 0.63 mg/kg (almost -6%) but not at other doses.

To summarize, the effects of NLX-112 in the different regions of interest were mostly obvious in the MCPO and the retrosplenial cortex in terms of BOLD increases. It also increased the BOLD signal in the dorsal thalamus, the colliculi and the cingulate cortex but this effect was non correlated to the dose. In terms of BOLD decrease, the effects were very significant both in the orbital cortex and the brainstem but varied in opposite ways as a function of dose.

2.2.2 NLX-101

The BOLD signal changes occurring after the injection of NLX-101 were quantified in the different regions of interest, and statistically compared to the changes occurring after the injection of NaCl 0.9% (Fig. 8). The highest positive BOLD responses were found in the magnocellular preoptic nuclei, with a BOLD signal increase of 7.6%, 6.5% and 7.2% at increasing doses. Other significant increases were found in the retrosplenial cortex (from 6.% at 0.16 mg/kg to 7.9% at 0.63 mg/kg) and the thalamus (from 5.3% at 0.16 mg/kg to 6.1% at 0.63 mg/kg). NLX-101 also induced a BOLD increase in the cingulate cortex at all doses (+3.2%, +3%, and +3.4%, respectively). Other significant increases were found in the colliculi at 0.32 mg/kg (+4.3%) and 0.63

mg/kg (+5.%). Significant decreases were detected in the brainstem, with an effect ranging from -4.8% at 0.32 mg/kg to -5.9 at 0.63 mg/kg. Other negative changes appeared in the orbital cortex but not at 0.32 mg/kg (effect between -4.7 and -4.1% at other doses).

To summarize, the effects of NLX-101 were most obvious in the MCPO, the retrosplenial cortex and dorsal thalamus in terms of BOLD increases, and in the brainstem in terms of BOLD decrease. Generally, the effect varied little with the dose but the highest dose tended to produce the highest changes.

NLX-112 and NLX-101 tended to produce similar regional effects in positive responses, but MCPO and retrosplenial cortex were more impacted by NLX-112. Furthermore, the effects of NLX-101 varied more consistently with the dose as compared to NLX-112. The negative effects of NLX-112 were more pronounced than NLX-101 in the orbital cortex and the brainstem, but for both drugs the dose effect was unclear in the orbital cortex.

2.2.3 NLX-112 vs NLX-101

The direct statistical comparisons of the effects produced by NLX-112 and NLX-101, as compared to their respective vehicle condition, showed that in the orbital cortex the BOLD signal decrease was more pronounced with NLX-112 than NLX-101 at 0.32 mg/kg ($p<0.05$), and in the hypothalamus the effects of NLX-112 and NLX-101 were significantly different at 0.63 mg/kg ($p<0.001$).

When comparing the time curves of BOLD signal, the effect of NLX-112 also tended to be more important in other regions such as the somatosensory cortex, although it was not significant (Fig. 8C-8E). The BOLD negative effects occurred generally slower than the BOLD increases, as shown in Fig. 8D and 8F, showing the effects of

NLX-101 and NLX-112 in the dorsal thalamus where the BOLD signal increased rapidly, just a few minutes after the injection.

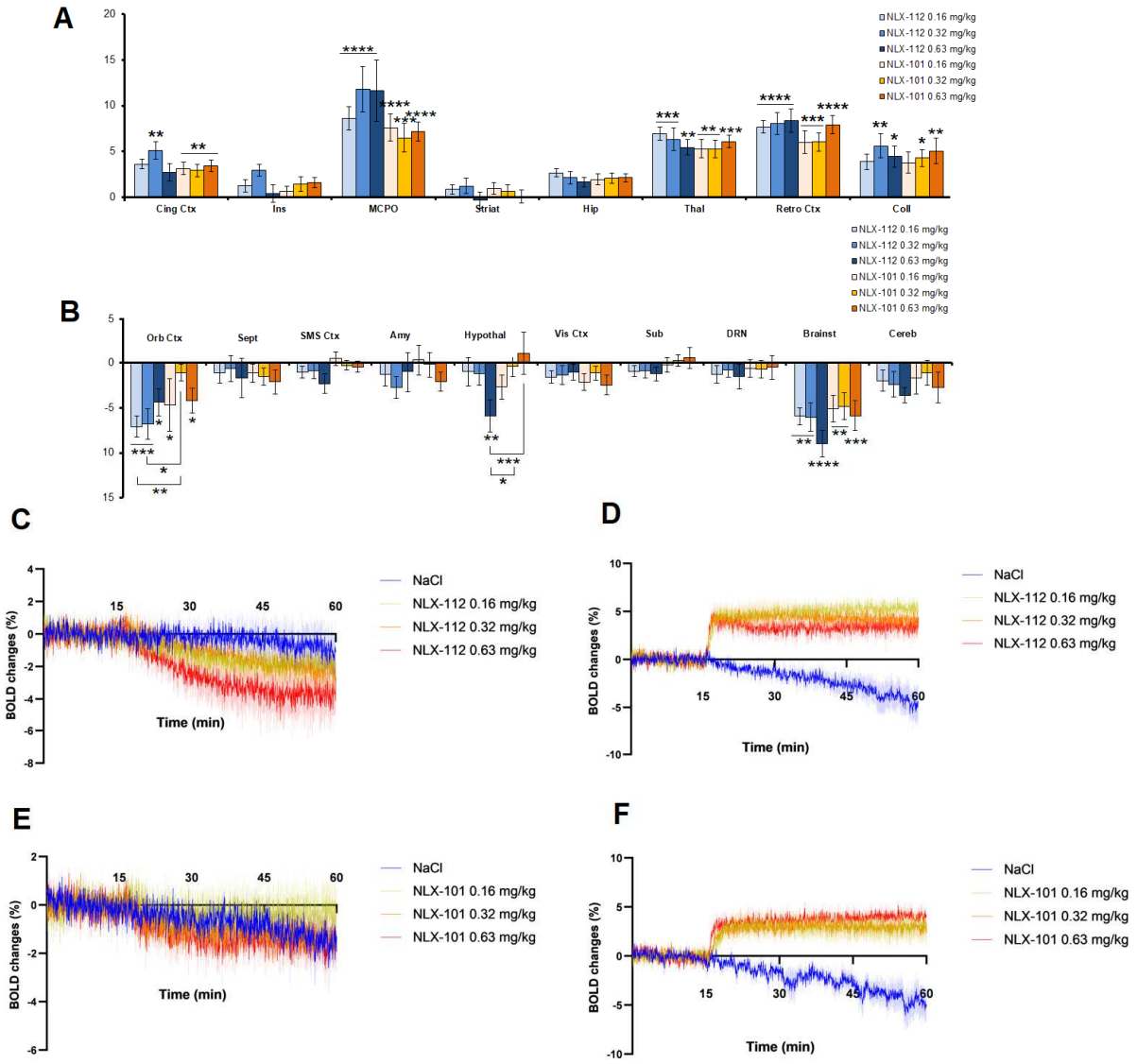

5-HT$_{1A}$ agonist	NLX-112			NLX-101		
Regions/Doses	0.16 mg/kg	0.32 mg/kg	0.63 mg/kg	0.16 mg/kg	0.32 mg/kg	0.63 mg/kg
Orb Ctx	**-7.10 ± 1.19 (***)**	**-6.80 ± 1.70 (***)**	**-4.38 ± 1.49 (*)**	**-4.68 ± 2.90 (*)**	-1.08 ± 0.95	**-4.18 ± 1.39 (*)**
Cing Ctx	3.61 ± 0.52	**5.08 ± 0.97 (**)**	2.71 ± 0.95	**3.15 ± 0.69 (**)**	**2.95 ± 0.67 (**)**	**3.41 ± 0.65 (**)**
Ins	1.25 ± 0.70	2.95 ± 0.62	0.42 ± 0.94	0.62 ± 0.58	1.45 ± 0.78	1.62 ± 0.54
MCPO	**8.62 ± 1.24 (****)**	**11.79 ± 2.45 (****)**	**11.66 ± 3.36 (****)**	**7.61 ± 1.44 (****)**	**6.50 ± 1.56 (***)**	**7.17 ± 1.04 (****)**
Sept	-1.08 ± 1.19	-0.59 ± 1.49	-1.70 ± 2.19	-1.12 ± 1.00	-1.52 ± 0.99	-2.12 ± 1.33
Striat	0.85 ± 0.52	1.22 ± 0.82	-0.31 ± 0.90	0.96 ± 0.67	0.67 ± 0.71	0.07 ± 0.70
Hip	2.66 ± 0.43	2.13 ± 0.67	1.68 ± 0.52	1.95 ± 0.58	2.05 ± 0.55	2.12 ± 0.43
SMS Ctx	-1.00 ± 0.65	-0.83 ± 0.92	-2.29 ± 1.10	0.49 ± 0.81	-0.26 ± 0.53	-0.42 ± 0.62
Amy	-1.25 ± 1.31	-2.73 ± 1.24	-0.96 ± 2.22	0.33 ± 1.71	-0.17 ± 1.41	-2.06 ± 1.06
Thal	**6.94 ± 0.72 (***)**	**6.33 ± 1.25 (***)**	**5.45 ± 0.83 (**)**	**5.27 ± 1.00 (**)**	**5.28 ± 0.98 (**)**	**6.08 ± 0.67 (***)**
Hypothal	-0.98 ± 1.61	-1.20 ± 1.28	**-5.90 ± 1.77 (**)**	-2.67 ± 1.35	-0.40 ± 1.07	1.15 ± 2.42
Retro Ctx	**7.68 ± 0.68 (****)**	**8.05 ± 1.22 (****)**	**8.40 ± 1.28 (****)**	**6.02 ± 1.22 (***)**	**6.03 ± 1.02 (***)**	**7.93 ± 0.98 (****)**
Coll	3.88 ± 0.86	**5.61 ± 1.30 (**)**	**4.43 ± 1.17 (*)**	3.78 ± 1.18	**4.29 ± 0.92 (*)**	**5.04 ± 1.39 (**)**
Vis Ctx	-1.57 ± 0.70	-1.35 ± 1.07	-1.04 ± 0.90	-2.13 ± 0.95	-1.12 ± 0.78	-2.46 ± 1.07
Sub	-0.94 ± 0.61	-0.84 ± 0.83	-1.23 ± 0.77	-0.22 ± 0.79	0.30 ± 0.67	0.58 ± 1.21
DRN	-1.27 ± 1.00	-0.75 ± 0.85	-1.52 ± 1.40	-0.65 ± 0.97	-0.73 ± 0.96	-0.46 ± 1.35
Brainst	**-5.93 ± 0.92 (**)**	**-6.02 ± 1.58 (**)**	**-8.99 ± 1.48 (****)**	**-5.10 ± 1.46 (**)**	**-4.80 ± 1.47 (**)**	**-5.86 ± 1.67 (***)**
Cereb	-1.97 ± 1.18	-2.39 ± 1.42	-3.60 ± 0.83	-1.68 ± 1.75	-1.11 ± 1.41	-2.72 ± 1.73

2.3 Functional connectivity

Correlation matrices were generated from the BOLD signal curves extracted in the regions of interest (Fig. 9A). Each correlation matrix corresponding to a given dose of agonist was compared to the injection of saline to facilitate the interpretation of results. The significant ($p<0.001$) changes in correlation coefficient compared to control (after Fisher transformation of correlation coefficients "r" into their respective values of inverse hyperbolic tangent "z") are represented in Figure 9B.

NLX-112 produced numerous changes in functional connectivity at all doses. Strong decreases of connectivity were found between the orbital cortex and the thalamus (from Δz=--1.2 at 0.16 mg/kg to -0.7 at 0.63 mg/kg) or the retrosplenial cortex (from

Δz=-1.0 at 0.16 mg/kg toΔz=-0.7 at 0.63 mg/kg) and between the septum and the thalamus (Δz=-1.2, -0.7 and -0.8 at the respective increasing doses) and the retrosplenial cortex (from Δz=-1.0 to Δz=-0.8). Connectivity was also decreased between the striatum and the retrosplenial cortex at 0.16 mg/kg and 0.63 mg/kg (Δz=-0.7). At 0.16 mg/kg and 0.32 mg/kg specifically, other significant decreases of connectivity were found between the orbital cortex and MCPO (Δz= -0.7 and -0.9), the cingulate cortex and the septum (Δz= -0.9 and -0.8), and between the MCPO and the septum (Δz= -0.8 for both doses). Other decreases were found between the hippocampus and orbital cortex (Δz= -0.9), the septum and hippocampus (Δz= -0.8), and the striatum and thalamus (Δz= -0.7) at 0.16 mg/kg only, and between the insula and the septum at 0.32 mg/kg only (Δz= -0.7). Increases of connectivity were also induced by NLX-112 between the amygdala and the thalamus at 0.16 mg/kg (Δz=+0.8), the amygdala and the retrosplenial cortex at 0.16 mg/kg and 0.32 mg/kg (Δz=+0.7 for both doses), the amygdala and the MCPO at 0.32 mg/kg and 0.63 mg/kg (Δz=+0.8 and 0.9), and the amygdala and cingulate cortex at 0.32 mg/kg (Δz=+0.7). At 0.63 mg/kg, connectivity of the brainstem was increased with the orbital cortex (Δz= +0.8), the cingulate cortex (Δz=+0.7), and the striatum (Δz=+0.7).

Globally, NLX-101 produced much less changes in connectivity than NLX-112 (Fig. 9). At all doses, the connectivity was decreased between the retrosplenial cortex and the orbital cortex (Δz=-0.7, Δz=-0.7 and Δz=-1.1 at 0.16 mg/kg, 0.32 mg/kg and 0.63 mg/kg, respectively) or the septum (Δz=-0.6, Δz=-0.7 and Δz=-1.0 at increasing doses), and between the septum and the thalamus (Δz=-0.6, Δz=-0.7 and Δz=-0.8 at increasing doses). The connectivity between the cingulate cortex and the septum was also decreased at 0.16 mg/kg and 0.63 mg/kg (Δz= -0.6). At 0.63 mg/kg, the functional connectivity was also decreased between the orbital cortex and the

thalamus (Δz=-0.9) or the MCPO (Δz=-0.6), between the striatum and the colliculi (Δz=-0.7), the thalamus (Δz= -0.8), and the retrosplenial cortex (Δz= -0.9), and between the cingulate cortex and the retrosplenial cortex (Δz= -0.6). No significant increase of connectivity was found at any dose of NLX-101.

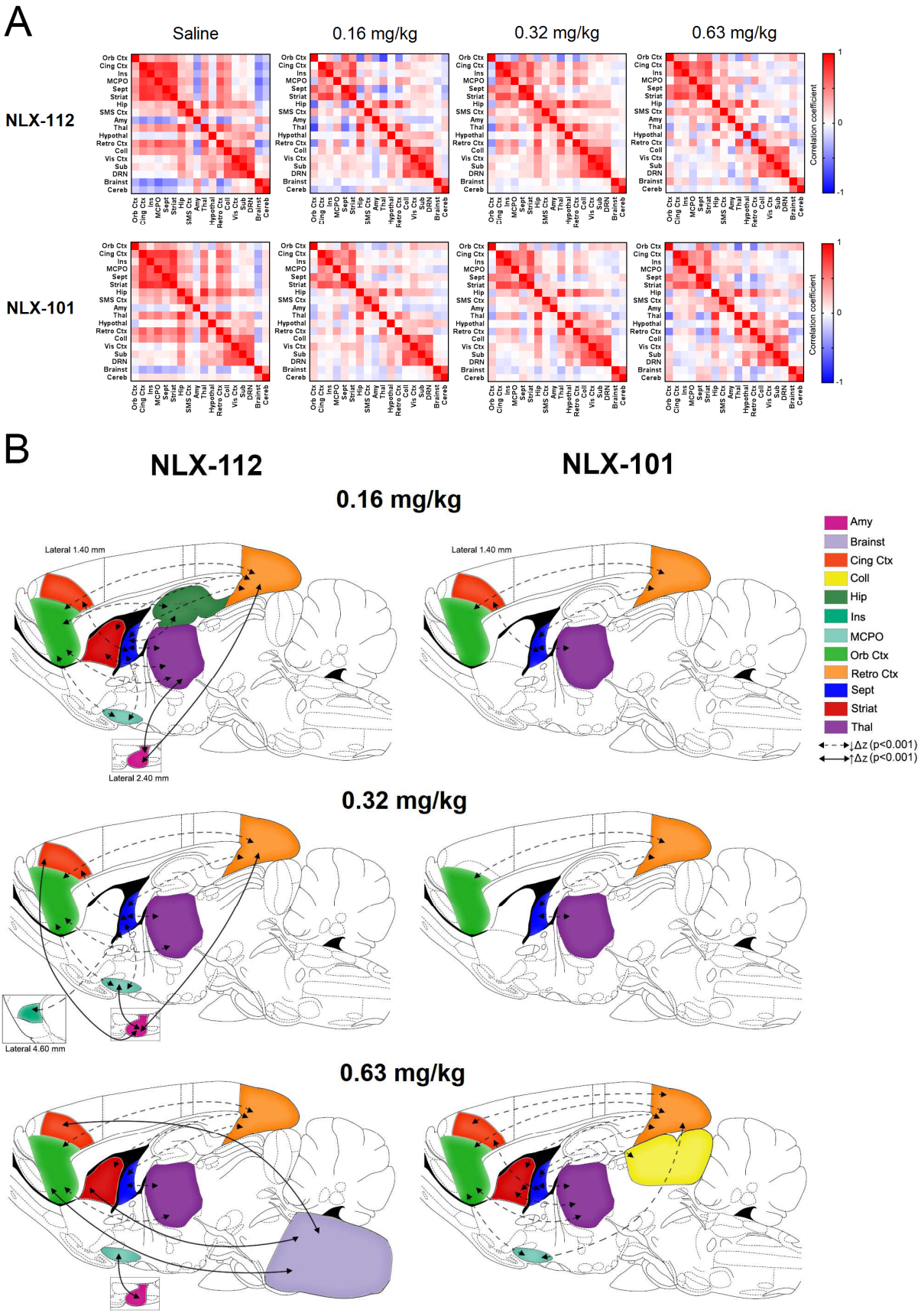
A
Saline
0.16 mg/kg
0.32 mg/kg
0.63 mg/kg
NLX-112
NLX-101
Orb Ctx
Cing Ctx
Ins
MCPO
Sept
Striat
Hip
SMS Ctx
Amy
Thal
Hypothal
Retro Ctx
Coll
Vis Ctx
Sub
DRN
Brainst
Cereb
Correlation coefficient
1
0
-1
B
NLX-112
NLX-101
0.16 mg/kg
0.32 mg/kg
0.63 mg/kg
Lateral 1.40 mm
Lateral 2.40 mm
Lateral 4.60 mm
Amy
Brainst
Cing Ctx
Coll
Hip
Ins
MCPO
Orb Ctx
Retro Ctx
Sept
Striat
Thal
↓Δz (p<0.001)
↑Δz (p<0.001)

3. Discussion

3.1 Study context and methodology

Pharmaco-MRI (phMRI) constitutes a promising tool to study serotonergic neurotransmission in animal models as well as in humans (Martin and Sibson, 2008; Anderson, 2008) and offers the opportunity to non-invasively explore the concept of biased agonism *in vivo*, an attractive prospect because few methodologies are available for translational studies of functional selectivity (Kenakin and Christopoulos, 2013; Zhou and Bohn, 2014). Here we focused on two close structural analogs, NLX-101 and NLX-112, that are both full agonists with a comparable affinity for 5-HT_{1A} receptors but differing in terms of intracellular signaling *in vitro* and regional targeting *in vivo* (Newman-Tancredi, 2011). The drugs were administered at the doses of 0.16/0.32/0.63 mg/kg, as their pharmacological effects are well documented at these doses in rats (Llado-Pelfort et al., 2010; Buritova et al., 2009; Llado-Pelfort et al., 2012a; Newman-Tancredi et al., 2009). Each animal was its own control and received each of the three doses of the agonist and the saline solution in a randomized order. The interval between two acquisitions was at least three days, to ensure complete elimination of the molecules (half-life of NLX-112 is about 1 to 2h – Bardin et al., 2005). The injected volumes were standardized at 600 µL and body temperature, cardiac and respiratory rates were monitored during the scans.

3.2 Global effects of NLX-112 and NLX-101

Some general remarks can be made before discussing in detail the different BOLD patterns.

Firstly, both agonists produced positive and negative BOLD signal changes, depending on the regions considered. Although it is difficult to interpret negative BOLD signal in fMRI studies (Lauritzen et al., 2012), they are rather commonly observed (Jenkins, 2012), and complex response patterns including BOLD inhibition may be expected in view of the great diversity of neurons expressing 5-HT_{1A} receptors (especially glutamatergic and GABAergic neurons which produce opposite effects in the brain) and the fact that 5-HT_{1A} receptors are coupled with inhibitory G proteins (Polter and Li, 2010). Previous studies showed decreases in relative cerebral blood volumes (rCBV) following injection of the 5-HT_{1A} agonist 8-OH-DPAT in 5-HT_{1A}-rich regions (Scanley et al., 2001; Gozzi et al., 2010; Mueggler et al., 2011; Razoux et al., 2013). Although these studies did not report positive effects of 8-OH-DPAT in physiological conditions, the BOLD signal is only indirectly related to cerebral blood flow and also depends on the cerebral metabolic rate of oxygen, two processes that can vary differently (Lauritzen et al., 2012). This may explain why BOLD increases were observed in this study and in other studies focusing on 5-HT_7 receptors but also using 8-OH-DPAT (Canese et al., 2011).

Secondly, the present study revealed that the effects of both molecules were generally more accentuated 30 to 60 minutes after drug administration. This is in agreement with previous studies showing that the changes in phosphorylated ERK 1/2 levels induced by NLX-101 or NLX-112 are higher 30 minutes after intraperitoneal drug administration (Buritova et al., 2009; Newman Tancredi et al., 2009). In fact, it would probably require several hours to measure the entire functional profile of these drugs because, in certain regions, changes in phosphorylated ERK 1/2 produced by NLX-112 remain maximal after one hour (Buritova et al., 2009), and in microdialysis studies maximal changes in dopamine or serotonin levels induced by both agonists

are reached in about 45 minutes and last more than two hours (Llado-Pelfort et al., 2010; Llado-Pelfort et al., 2012a). Micro-positron emission tomography (PET) studies using radiolabeled [^{18}F]NLX-112 and [^{18}F]NLX-101 also show that their dissociation from 5-HT$_{1A}$ receptors is very slow (Lemoine et al., 2010; Vidal et al., 2018a). It would be technically difficult to analyze drug effects on BOLD signal for longer periods in view of the volume of information generated by the phMRI acquisitions, and the fact that animals would be anesthetized during several hours. However, it is likely that the most pronounced effects of the agonists are indeed observed under present conditions, as previous studies found that their maximal responses were reached between 30 and 60 minutes after drug administration (Buritova et al., 2009; Newman-Tancredi et al., 2009).

Thirdly, the BOLD signal changes induced by the drugs were not necessarily proportional to the dose, an important consideration that was already reported in other phMRI studies (Steward et al., 2005). These results underline the importance of using several doses to fully characterize drugs effects in a phMRI protocol.

Despite some shared properties, the results tend to show that NLX-101 and NLX-112 display preferences for activation of different populations of 5-HT$_{1A}$ receptors and/or different signaling pathways. Among the main differences, NLX-112 produced stronger BOLD increases in the MCPO, and more widespread negative effects, with pronounced decreases in the brainstem and the orbital cortex compared to NLX-101. Interestingly, the voxel analysis did not show any effect of NLX-101 in the dorsal raphe at any dose, consistently with previously published results (Newman-Tancredi et al., 2009; Llado-Pelfort et al., 2010), whereas an inhibitory effect of NLX-112 in the dorsal raphe nucleus was directly observed, although only at 0.32 mg/kg. In more caudal parts of the brainstem that contain other raphe nuclei, NLX-112 also

decreased the BOLD signal at all doses whereas the effect was non-significant for NLX-101. NLX-101 and NLX-112 also had distinct functional connectivity profiles: the effects of NLX-112 were complex, with many increases or decreases in connectivity compared to control, whereas NLX-101 only induced decreases restricted to certain pairs of regions. Finally, direct statistical comparisons between the respective effects of NLX-112 and NLX-101 show that they produce distinct functional responses at equal doses, and especially at the lowest dose we tested, consistent with the hypothesis that the regional selectivity of NLX-101 is optimal at low doses. In vivo biased agonism of NLX-101 seems therefore to be a dose-dependent mechanism, which is also consistent with our previous PET-fMRI study in cat brain (Vidal et al, 2018b). Overall, the present observations support the view that the agonists preferentially stimulate different populations of 5-HT_{1A} receptors, as discussed previously for these compounds (Llado-Pelfort et al., 2010; Llado-Pelfort et al., 2012a).

3.3 BOLD patterns interpretation

In the lateral septum , the dorsal raphe (for NLX-112) or the somatosensory cortex, the BOLD signal decrease may be directly due to the stimulation of target receptors that are known to be expressed in those regions, given that 5-HT_{1A} receptors are inhibitory and induce a fast hyperpolarization of neurons through GIRK channel activation. In previous studies, 8-OH-DPAT was also reported to induce rCBV decreases in these areas rich in 5-HT_{1A} receptors (Scanley et al., 2001; Gozzi et al., 2010; Mueggler et al., 2011; Razoux et al., 2013). On the contrary, in the cingulate cortex, which is also rich in 5-HT_{1A} receptors, both molecules tended to increase the BOLD signal. This could be due to the fact that in this region, activation of 5-HT_{1A} receptors has been shown to induce a local liberation of dopamine (Llado-Pelfort et

al., 2012b; Newman-Tancredi, 2011), which is known to increase the BOLD signal (Jenkins, 2012). The BOLD increase in the cingulate cortex might therefore be related to an increase of dopamine release in this region, or to different transduction mechanisms compared to other cortical regions. In our study, the effects of NLX-101 or NLX-112 were not systematically observed across the different doses (and in particular, not for the highest dose of NLX-112), which could be due to opposite effects of the agonist direct stimulation of local 5-HT_{1A} receptors and indirect effects regarding the release of dopamine. Moreover, as different populations of neurons express 5-HT_{1A} receptors in the cortex (Santana et al., 2004), namely GABAergic interneurons and glutamatergic pyramidal neurons, 5-HT_{1A} receptor stimulation by agonists could induce mixed effects, depending on the proportion of interneurons or pyramidal neurons targeted (Llado-Pelfort et al., 2012b).

Both NLX-101 and NLX-112 induced a strong increase of BOLD signal at every dose, starting from the habenula back to the colliculi, reaching also the posterior parts of the retrosplenial cortex and the dorsal part of the thalamus. These results are quite puzzling considering that these regions are not known as particularly rich in 5-HT_{1A} receptors. Nevertheless, these regions and in particular the dorsal thalamus are strongly labeled by [^{18}F]NLX-112 and [^{18}F]NLX-101 in microPET experiments in rats, suggesting they contain highly functional populations of 5-HT_{1A} receptors.

Focusing on the main differences between NLX-101 and NLX-112, it appears that the effects of NLX-101 in terms of BOLD increase were generally comparable to those of NLX-112: the same important cluster in the dorsal thalamus and colliculi was observed, with a lower maximal effect in the posterior retrosplenial cortex. In the cingulate cortex, the effects of both molecules were also comparable, although increasing the dose of NLX-112 tended to reduce the positive response, whereas the

BOLD increase were similar across the three doses for NLX-101. In the magnocellular preoptic nuclei however, the effect of NLX-112 was higher than NLX-101, as shown by the ROIs analysis. Interestingly, the local expression of 5-HT_{1A} receptors in the magnocellular preoptic area has been previously shown in rat, and such receptors may be of functional importance for numerous hypothalamic functions (Marvin et al., 2010).

In terms of negative BOLD responses, the effects of NLX-101 were generally weaker than NLX-112. The voxel based analysis suggested that the effects of NLX-112 were spatially more extended than NLX-101, for instance in regions like the somatosensory cortex, the lateral septum and the subiculum. In the brainstem and the orbital cortex, both the voxel analysis and the ROIs analysis clearly showed that the effect of NLX-101 was much less pronounced that NLX-112.

The dorsal raphe, which is of critical importance in the serotonergic system, did not display any significant effect of NLX-101, contrary to NLX-112. This is consistent with previous work showing that NLX-101 produces a significant effect on c-Fos expression in the dorsal raphe at 0.63 mg/kg but not 0.16 mg/kg (Newman-Tancredi et al., 2009). Furthermore, NLX-101 decreased ERK phosphorylation in the hippocampus at 0.63 mg/kg and not at 0.16 mg/kg, which was interpreted as being a consequence of decreased serotonin release due to the stimulation of 5-HT_{1A} autoreceptors in the dorsal raphe (Newman-Tancredi et al., 2009). Conversely, NLX-112 produces a strong decrease of ERK phosphorylation in hippocampus at 0.16 mg/kg, suggesting that it exerts a potent action at 5-HT_{1A} autoreceptors (Buritova et al., 2009). Microdialysis studies also showed that NLX-112 inhibits serotonin release in the hippocampus at low doses (ED_{50}=0.09 mg/kg; Llado-Pelfort et al., 2012a) whereas higher doses of NLX-101 are required (ED_{50}=0.24 mg/kg; Llado-Pelfort et

al., 2010). However, one should be careful when interpreting these results, given that the effect of NLX-112 in the dorsal raphe was only clearly observed at 0.32 mg/kg. The signal to noise ratio in the raphe might be too low to reliably detect the potential effects of the molecules.

In the caudal brainstem, the wide and strong decrease we observed with NLX-112 was unexpected as it is a region that is not usually described as rich in 5-HT_{1A} receptors, apart from the medial part that contains the caudal raphe nuclei such as raphe obscurus and raphe magnus. However, this whole region is heavily labeled by [^{18}F]NLX-112 and [^{18}F]NLX-101 in microPET experiments in rat brain (Lemoine et al., 2010; Vidal et al., 2018a), which suggests the presence of highly functional 5-HT_{1A} receptors in many regions of the brainstem that might be involved in the pro-respiratory properties of these agonists (Levitt et al., 2013; Ren et al., 2015) and the antinociceptive properties of NLX-112 (Colpaert et al., 2002; Buritova et al., 2005; Newman-Tancredi et al., 2018). Contrary to the region-based analysis, the effect of NLX-101 in the brainstem was not detected in the voxel analysis, whereas it was observed for all three doses of NLX-112. The weaker effect of NLX-101 on presynaptic receptors could be linked to this observation, although the raphe nuclei present in this part of the brainstem are only located at the medial parts.

Other important differences were found in the frontal orbital cortex, where the BOLD signal decrease was observed for every dose of NLX-112 but only appeared at 0.63 mg/kg of NLX-101. This might be of critical importance for the favorable profile NLX-101 on cognitive function in comparison to other 5-HT_{1A} agonists (Depoortère et al., 2010), and deserves further investigation.

A last difference between the two compounds, is the negative response that all doses of NLX-112 produced in the ventral and lateral parts of the striatum, but which were much weaker with NLX-101 and only observed at one dose. Such effects might be related to the strong antidyskinetic properties of NLX-112 (Iderberg et al., 2015) and also warrant further studies.

Finally, an important consideration is that the modulation of 5-HT release through activation of 5-HT_{1A} autoreceptors may have considerable effects on the BOLD signal in multiple brain areas. This could account for the wider effects of NLX-112 across the brain, with some that could be related to the inhibition of 5-HT neurons after targeting of 5-HT_{1A} receptors in raphe nuclei. In comparison, the increased 5-HT release induced by fenfluramine in halothane-anesthetized rats produced substantial BOLD signal changes in the frontal and orbital cortex, which were also associated with changes in c-Fos expression (Preece et al., 2009). A decrease of endogenous 5-HT release in this region elicited by 5-HT_{1A} autoreceptor stimulation may therefore be important for the interpretation of the present data. However the global influence of 5-HT_{1A} agonists and particularly NLX-112 on the serotonergic system and subsequent changes in BOLD signal may be much more extensive, given the wide distribution of the serotonergic projections, that are present even in the brainstem and between the different raphe nuclei (Hensler, 2006).

3.4 Functional connectivity changes

A different manner to understand the effect of central drugs using fMRI is to evaluate how the time fluctuations of the signal are correlated between different pairs of regions using functional connectivity analysis. Such approaches have been very useful to evaluate the global effects of molecules such as 5-HT_{1A} ligands on cerebral

networks (Razoux et al., 2013). We therefore also analyzed our data using this approach, with the hypothesis that NLX-101 and NLX-112 would produce different changes in functional connectivity due to the preferential targeting of different regions.

As expected, NLX-101 and NLX-112 produced distinctive changes of functional connectivity. In general, both agonists induced a decrease of connectivity between several brain regions as compared to the saline injection. Systematic decreases for both molecules were observed between the orbital cortex and the retrosplenial cortex, between the septum and the retrosplenial cortex, and between the septum and the thalamus. Those regions appeared thus as important hubs in the modulation of functional connectivity through 5-HT_{1A} agonists and were also associated to a decrease of connectivity with other areas (for instance, with MCPO and cingulate cortex for the septum for certain doses of NLX-112).

NLX-112 also induced some increases in connectivity with the amygdala and or brainstem, contrary to NLX-101 that never induced any significant increase. On the contrary, increasing the dose of NLX-101 tended to produce more different temporal responses across the different regions. This is consistent with the reported biased properties of the molecule, as selective targeting of only few populations of 5-HT_{1A} receptors would be expected to produce different regional responses as opposed to a global response that may be produced when activating indifferently these receptors across the whole brain.

The two drugs profiles were therefore very different in terms of functional connectivity, and this type of analysis seems a promising approach to investigate and compare the global effects of different compounds.

3.4 Limitations and perspectives

Some technical aspects should be considered in the context of the present study. Anesthesia can modify neuronal activity, metabolism, vascular reactivity and neurovascular coupling (Jenkins, 2012). The magnitude of these non-specific effects is difficult to estimate but they can directly impact neurotransmission. Although there is no ideal anesthetic, we chose to use isoflurane as it is the most often used in phMRI studies (Haensel et al., 2015). Moreover, we used strictly the same anesthesia protocol in all acquisitions, ensuring comparability between the studied agonists. In a more general manner, phMRI does not provide direct information about the receptors primarily targeted by the ligands. Therefore, the BOLD patterns observed in our study could be due to indirect effects on other neurons than those expressing 5-HT_{1A} receptors. This must be kept in mind when interpreting the results, especially because 5-HT_{1A} autoreceptors can modulate endogenous serotonin release, which is likely to modify BOLD signal in serotonergic projection areas (Preece et al., 2009; McKie et al., 2005; Jenkins, 2012). Furthermore, 5-HT_{1A} agonists might have peripheral effects on the vascular tone that would impact the BOLD signal, also the effect of 5-HT_{1A} receptor stimulation on blood vessels is not clearly characterized. Another possible limitation is the potential induction of peripheral effects by 5-HT_{1A} agonists on respiratory and cardiac function. Here, heart rate was monitored for certain animals and we did not detect any significant change after NLX-112 or NLX-101 administration. However, the molecules did produce some transient effects on the respiration, and we therefore used the respiratory rate as a regressor in the voxel based analysis. A last limitation is that the plasmatic concentration of the drugs could have been used to validate the good intraperitoneal injection and to evaluate the dose-effect of the agonists on the BOLD response as a function of changes in blood concentration. Nevertheless, despite these limitations,

the present study demonstrates that phMRI differentiates between two closely-related 5-HT_{1A} receptor agonists in terms of BOLD effect profiles and functional connectivity patterns, and raises the prospect of examining 'biased agonist' effects of NLX-101 and NLX-112 directly in human brain imaging studies.

Declarations of interest: A. Newman-Tancredi is an employee and stockholder of Neurolixis. The other authors have nothing to disclose.

Funding: This work was supported by the LABEX PRIMES (ANR-11-LABX-0063) of Université de Lyon and the program "Investissements d'Avenir" (ANR-11-IDEX-0007) operated by the French National Research Agency (ANR).

References

Anderson IM, McKie S, Elliott R, Williams SR, Deakin JF (2008) Assessing human 5-HT function in vivo with pharmacoMRI. Neuropharmacology 55, 1029-1037.

Andrade R, Huereca D, Lyons JG, Andrade EM, McGregor KM (2015) 5-HT1A Receptor-Mediated Autoinhibition and the Control of Serotonergic Cell Firing. ACS Chem Neurosci 6, 1110-1115.

Assie MB, Koek W (1996) Effects of 5-HT1A receptor antagonists on hippocampal 5-hydroxytryptamine levels: (S)-WAY100135, but not WAY100635, has partial agonist properties. Eur J Pharmacol 304, 15-21.

Bardin L, Assie MB, Pelissou M, Royer-Urios I, Newman-Tancredi A, Ribet JP, Sautel F, Koek W, Colpaert FC (2005) Dual, hyperalgesic, and analgesic effects of the high-efficacy 5-hydroxytryptamine 1A (5-HT1A) agonist F 13640 [(3-chloro-4-fluoro-phenyl)-[4-fluoro-4-{[(5-methyl-pyridin-2-ylmethyl)-amino]-me thyl}piperidin-1-yl]methanone, fumaric acid salt]: relationship with 5-HT1A receptor occupancy and kinetic parameters. J Pharmacol Exp Ther 312, 1034-1042.

Becker G, Bolbos R, Costes N, Redoute J, Newman-Tancredi A, Zimmer L (2016) Selective serotonin 5-HT1A receptor biased agonists elicit distinct brain activation patterns: a pharmacoMRI study. Sci Rep 6, 26633.

Berg KA, Clarke WP (2006) Development of functionally selective agonists as novel therapeutic agents. Drug Discov Today Ther Strateg 3, 421-428.

Birn RM, Murphy K, Handwerker DA, Bandettini PA, (2009) fMRI in the presence of task-correlated breathing variations. Neuroimage 47, 1092-1104.

Buritova J, Berrichon G, Cathala C, Colpaert F, Cussac D (2009) Region-specific changes in 5-HT1A agonist-induced Extracellular signal-Regulated Kinases 1/2 phosphorylation in rat brain: a quantitative ELISA study. Neuropharmacology 56, 350-361.

Buritova J, Larrue S, Aliaga M, Besson JM, Colpaert F (2005) Effects of the high-efficacy 5-HT1A receptor agonist, F 13640 in the formalin pain model: a c-Fos study. Eur J Pharmacol 514, 121-130.

Canese R, Marco EM, De Pasquale F, Podo F, Laviola G, Adriani W (2011) Differential response to specific 5-Ht(7) versus whole-serotonergic drugs in rat forebrains: a phMRI study. Neuroimage 58, 885-894.

Colpaert, FC, Tarayre JP, Koek W, Pauwels PJ, Bardin L, Xu XJ, Wiesenfeld-Hallin Z, Cosi C, Carilla-Durand E, Assie MB, Vacher B (2002) Large-amplitude 5-HT1A receptor activation: a new mechanism of profound, central analgesia. Neuropharmacology 43, 945-958.

Depoortere R, Auclair AL, Bardin L, Colpaert FC, Vacher, B, Newman-Tancredi A (2010) F15599, a preferential post-synaptic 5-HT1A receptor agonist: activity in models of cognition in comparison with reference 5-HT1A receptor agonists. Eur Neuropsychopharmacol 20, 641-654.

Gozzi A, Jain A, Giovannelli A, Bertollini C, Crestan V, Schwarz AJ, Tsetsenis T, Ragozzino D, Gross CT, Bifone A (2010) A neural switch for active and passive fear. Neuron 67, 656-666.

Haensel JX, Spain A, Martin C (2015) A systematic review of physiological methods in rodent pharmacological MRI studies. Psychopharmacology (Berl) 232, 489-499.

Hensler, J G (2006) Serotonergic modulation of the limbic system. Neurosci Biobehav Rev 30, 203-214.

Iderberg H, McCreary AC, Varney MA, Kleven MS, Koek W, Bardin L, Depoortere R, Cenci MA, Newman-Tancredi A (2015) NLX-112, a novel 5-HT1A receptor agonist for the treatment of L-DOPA-induced dyskinesia: Behavioral and neurochemical profile in rat. Exp Neurol 271, 335-350.

Jenkins BG (2012) Pharmacologic magnetic resonance imaging (phMRI): imaging drug action in the brain. Neuroimage 62, 1072-1085.

Kenakin T, Christopoulos A (2013) Signalling bias in new drug discovery: detection, quantification and therapeutic impact. Nat Rev Drug Discov 12, 205-216.

Kerr CW, Bishop GA (1992) The physiological effects of serotonin are mediated by the 5HT1A receptor in the cat's cerebellar cortex. Brain Res 591, 253-260.

Lacivita E, Di Pilato P, De Giorgio P, Colabufo NA, Berardi F, Perrone R, Leopoldo M (2012) The therapeutic potential of 5-HT1A receptors: a patent review. Expert Opin Ther Pat 22, 887-902.

Lancelot S, Roche R, Slimen A, Bouillot C, Levigoureux E, Langlois JB, Zimmer L, Costes N (2014) A multi-atlas based method for automated anatomical rat brain MRI segmentation and extraction of PET activity. PLoS One 9, e109113.

Lanfumey L, Hamon M (2000) Central 5-HT(1A) receptors: regional distribution and functional characteristics. Nucl Med Biol 27, 429-435.

Lauritzen M, Mathiesen C, Schaefer K, Thomsen KJ (2012) Neuronal inhibition and excitation, and the dichotomic control of brain hemodynamic and oxygen responses. Neuroimage 62, 1040-1050.

Lemoine L, Verdurand M, Vacher B, Blanc E, Le Bars D, Newman-Tancredi A, Zimmer L (2010) [18F]F15599, a novel 5-HT1A receptor agonist, as a radioligand for PET neuroimaging. Eur J Nucl Med Mol Imaging 37, 594-605.

Levitt ES, Hunnicutt BJ, Knopp SJ, Williams JT, Bissonnette JM (2013) A selective 5-HT1a receptor agonist improves respiration in a mouse model of Rett syndrome. J Appl Physiol (1985) 115, 1626-1633.

Llado-Pelfort L, Assie MB, Newman-Tancredi A, Artigas F, Celada P (2010) Preferential in vivo action of F15599, a novel 5-HT(1A) receptor agonist, at postsynaptic 5-HT(1A) receptors. Br J Pharmacol 160, 1929-1940.

Llado-Pelfort L, Assie MB, Newman-Tancredi A, Artigas F, Celada P (2012) In vivo electrophysiological and neurochemical effects of the selective 5-HT1A receptor agonist, F13640, at pre- and postsynaptic 5-HT1A receptors in the rat. Psychopharmacology (Berl) 221, 261-272.

Llado-Pelfort L, Santana N, Ghisi V, Artigas F, Celada P (2012) 5-HT1A receptor agonists enhance pyramidal cell firing in prefrontal cortex through a preferential action on GABA interneurons. Cereb Cortex 22, 1487-1497.

Luttgen M, Ogren SO, Meister B (2005) 5-HT1A receptor mRNA and immunoreactivity in the rat medial septum/diagonal band of Broca-relationships to GABAergic and cholinergic neurons. J Chem Neuroanat 29, 93-111.

Mandeville JB, Liu CH, Vanduffel W, Marota JJ, Jenkins BG (2014) Data collection and analysis strategies for phMRI. Neuropharmacology 84, 65-78.

Mannoury la Cour C, El Mestikawy S, Hanoun N, Hamon M, Lanfumey L (2006) Regional differences in the coupling of 5-hydroxytryptamine-1A receptors to G proteins in the rat brain. Mol Pharmacol 70, 1013-1021.

Martin C, Sibson NR (2008) Pharmacological MRI in animal models: a useful tool for 5-HT research? Neuropharmacology 55, 1038-1047.

Marvin E, Scrogin K, Dudás B (2010) Morphology and distribution of neurons expressing serotonin 5-HT_{1A} receptors in the rat hypothalamus and the surrounding diencephalic and telencephalic areas. J Chem Neuroanat 39, 235-241.

McCreary AC, Varney MA, Newman-Tancredi A (2016) The novel 5-HT1A receptor agonist, NLX-112 reduces l-DOPA-induced abnormal involuntary movements in rat: A chronic administration study with microdialysis measurements. Neuropharmacology 105, 651-660.

McKie S, Del-Ben C, Elliott R, Williams S, del Vai N, Anderson I, Deakin JF (2005) Neuronal effects of acute citalopram detected by pharmacoMRI. Psychopharmacology (Berl) 180, 680-686.

Mogha A, Guariglia SR, Debata PR, Wen GY, Banerjee P (2012) Serotonin 1A receptor-mediated signaling through ERK and PKCα is essential for normal synaptogenesis in neonatal mouse hippocampus. Transl Psychiatry 2, e66.

Montalbano A, Corradetti R, Mlinar B (2015) Pharmacological Characterization of 5-HT1A Autoreceptor-Coupled GIRK Channels in Rat Dorsal Raphe 5-HT Neurons. PLoS One 10, e0140369.

Mueggler T, Razoux F, Russig H, Buehler A, Franklin TB, Baltes C, Mansuy IM, Rudin M (2011) Mapping of CBV changes in 5-HT(1A) terminal fields by functional MRI in the mouse brain. Eur Neuropsychopharmacol 21, 344-353.

Newman-Tancredi A, Martel JC, Assie MB, Buritova J, Lauressergues E, Cosi C, Heusler P, Bruins Slot L, Colpaert FC, Vacher B, Cussac D (2009) Signal transduction and functional selectivity of F15599, a preferential post-synaptic 5-HT1A receptor agonist. Br J Pharmacol 156, 338-353.

Newman-Tancredi A, Martel JC, Cosi C, Heusler P, Lestienne F, Varney MA, Cussac D (2017) Distinctive in vitro signal transduction profile of NLX-112, a potent and efficacious serotonin 5-HT1A receptor agonist. J Pharm Pharmacol 69, 1178-1190.

Newman-Tancredi A, Bardin L, Auclair A, Colpaert F, Depoortère R, Varney MA (2018) NLX-112, a highly selective 5-HT1A receptor agonist, mediates analgesia and antidepressant-like activity in rats via spinal cord and prefrontal cortex 5-HT1A receptors, respectively. Brain Res 1688,1-7.

Newman-Tancredi A (2011) Biased agonism at serotonin 5-HT1A receptors: preferential postsynaptic activity for improved therapy of CNS disorders. Neuropsychiatry 1, 149-164.

Polter AM, Li X, (2010) 5-HT1A receptor-regulated signal transduction pathways in brain. Cell Signal 22, 1406-1412.

Preece MA, Taylor MJ, Raley J, Blamire A, Sharp T, Sibson NR (2009) Evidence that increased 5-HT release evokes region-specific effects on blood-oxygenation level-dependent functional magnetic resonance imaging responses in the rat brain. Neuroscience 159, 751-759.

Razoux F, Baltes C, Mueggler T, Seuwen A, Russig H, Mansuy I, Rudin M (2013) Functional MRI to assess alterations of functional networks in response to pharmacological or genetic manipulations of the serotonergic system in mice. Neuroimage 74, 326-336.

Ren J, Ding X, Greer JJ (2015) 5-HT1A receptor agonist Befiradol reduces fentanyl-induced respiratory depression, analgesia, and sedation in rats. Anesthesiology 122, 424-434.

Santana N, Bortolozzi A, Serrats J, Mengod G, Artigas F (2004) Expression of serotonin1A and serotonin2A receptors in pyramidal and GABAergic neurons of the rat prefrontal cortex. Cereb Cortex 14, 1100-1109.

Scanley BE, Kennan RP, Gore JC (2001) Changes in rat cerebral blood volume due to modulation of the 5-HT(1A) receptor measured with susceptibility enhanced contrast MRI. Brain Res 913, 149-155.

Steward CA, Marsden CA, Prior MJ, Morris PG, Shah YB (2005) Methodological considerations in rat brain BOLD contrast pharmacological MRI. Psychopharmacology (Berl) 180, 687-704.

Vidal B, Fieux S, Colom M, Billard T, Bouillot C, Barret O, Constantinescu C, Tamagnan G, Newman-Tancredi A, Zimmer L (2018) 18F-F13640 preclinical evaluation in rodent, cat and primate as a 5-HT1A receptor agonist for PET neuroimaging. Brain Struct Funct 223(6):2973-2988.

Vidal B, Fieux S, Redouté J, Villien M, Bonnefoi F, Le Bars D, Newman-Tancredi A, Costes N, Zimmer L (2018) In vivo biased agonism at 5-HT1A receptors: characterisation by simultaneous PET/MR imaging. Neuropsychopharmacology 43(11):2310-2319.

Zhou L, Bohn LM (2014) Functional selectivity of GPCR signaling in animals. Curr Opin Cell Biol 27, 102-108.

Figure legends

Figure 1: Significant BOLD changes following i.p injection of NLX-112 at 0.16 mg/kg in rat brain ($p<0.001$), during three successive time-ranges of 15 minutes (T1 to T3). T scores in color scales (BOLD increases in red/yellow, BOLD decreases in blue).

Figure 2: Significant BOLD changes following i.p injection of NLX-112 at 0.32 mg/kg in rat brain ($p<0.001$), during three successive time-ranges of 15 minutes (T1 to T3). T scores in color scales (BOLD increases in red/yellow, BOLD decreases in blue).

Figure 3: Significant BOLD changes following i.p injection of NLX-112 at 0.63 mg/kg in rat brain ($p<0.001$), during three successive time-ranges of 15 minutes (T1 to T3). T scores in color scales (BOLD increases in red/yellow, BOLD decreases in blue).

Figure 4: Significant BOLD changes following i.p injection of NLX-101 at 0.16 mg/kg in rat brain ($p<0.001$), during three successive time-ranges of 15 minutes (T1 to T3). T scores in color scales (BOLD increases in red/yellow, BOLD decreases in blue).

Figure 5: Significant BOLD changes following i.p injection of NLX-101 at 0.32 mg/kg in rat brain ($p<0.001$), during three successive time-ranges of 15 minutes (T1 to T3). T scores in color scales (BOLD increases in red/yellow, BOLD decreases in blue).

Figure 6: Significant BOLD changes following i.p injection of NLX-101 at 0.63 mg/kg in rat brain ($p<0.001$), during three successive time-ranges of 15 minutes (T1 to T3). T scores in color scales (BOLD increases in red/yellow, BOLD decreases in blue).

Figure 7: Significant differences between BOLD changes induced by NLX-101 or NLX-112 at equal doses ($p<0.001$), from 30 to 45 minutes post-injection. T scores in color scales (BOLD signal higher for NLX-112 than NLX-101 in green, BOLD signal higher for NLX-101 than NLX-112 in purple).

Figure 8: BOLD signal changes induced by NLX-112 and NLX-101 in rat brain, expressed as percentages compared to control (mean ± SEM). **A** = Positive effects; **B** = Negative effects. Amy = Amygdala; Brainst = Brainstem; Cereb = Cerebellum; Cing Ctx = Cingulate cortex; Coll = Colliculus; Dors Thal = Dorsal thalamus; DRN = Dorsal raphe nucleus; Hip = Hippocampus; Hyp = Hypothalamus; Ins = Insula; MCPO = Magnocellular preoptic nuclei; Orb Ctx = Orbital cortex; Retro Ctx = Retrosplenial cortex; Sept = Lateral septum; SMS Ctx = Somatosensory cortex; Striat = Striatum; Sub = Subiculum; Vis Ctx = Visual cortex. BOLD changes were compared to control using a two-way ANOVA followed by a Bonferroni's post-hoc test ($p<0.05$). Respective effects of molecules in each region were compared at equal doses using a 2-way ANOVA followed by Tukey's post hoc tests($p<0.05$). Time courses of the BOLD signal changes following the injection of NLX-112 in the somatosensory cortex in **C** and in the dorsal thalamus in **D**, or following the injection of NLX-101 in the somatosensory cortex in **E** and the dorsal thalamus in **F**.

Figure 9: A: Functional connectivity analysis following injection of saline, NLX-112 or NLX-101 at increasing doses. The correlation matrices are expressed as mean values of Pearson correlation coefficient r. Negative values of correlation coefficient are shown in blue, and positive values of correlation coefficient are shown in red. The regions are presented in the rostro-caudal direction. **B:** Schematic representation of the significant changes in functional connectivity ($p<0.001$) as measured by comparing the correlation coefficient after Fisher transformation of r values into z values . The dashed arrows represent the significant decreases of functional connectivity between two regions and the solid arrows represent the significant increases of functional connectivity between two regions , as compared to the saline injection.

Table 1: BOLD signal changes induced by NLX-112 and NLX-101 in rat brain, expressed as percentages compared to control (mean differences from saline ± SEM). Amy = Amygdala; Brainst = Brainstem; Cereb = Cerebellum; Cing Ctx = Cingulate cortex; Coll = Colliculus; Dors Thal = Dorsal thalamus; DRN = Dorsal raphe nucleus; Hip = Hippocampus; Hyp =

Hypothalamus; Ins = Insula; MCPO = Magnocellular preoptic nuclei; Orb Ctx = Orbital cortex; Retro Ctx = Retrosplenial cortex; Sept = Lateral septum; SMS Ctx = Somatosensory cortex; Striat = Striatum; Sub = Subiculum; Vis Ctx = Visual cortex. BOLD changes were compared to control using a one-way ANOVA followed by a Dunnett's post-hoc test ($p<0.05$).